Implementation of Multi-Phase DC-DC Isolated Converter for Solar Applications

[1] Venkataramana Guntreddi; [2] B. Srinivasa Rao; [3] Jaganamohan Rao Tarra; [4] Kanaka Raju Kalla; [5] Krishna Mohan Tatikonda

[1] Associate Proff, School of Engineering and Applied Science, Kampala International University - Western Campus Bushenyi, Uganda

[2,3,4] Assistant Proff, Aditya Institute of Technology and Management, Tekkali, Srikakulam, Andhra Pradesh 532201, India

[5] Assistant Proff, Andhra Loyola Institute of Engineering & Technology, Vijayawada, Andhra Pradesh 520008, India

Corresponding Author: B. Srinivasa Rao

Abstract: Five-phase isolated DC-DC converters with bidirectional are suggested in this paper. In these converters, a three-level converter or a three-leg-controlled rectifier is coupled to a multi-level modified converter via a high frequency transformer. Better voltage and current waveforms can be obtained on the transformer's primary and secondary sides by employing a 5-level converter, which will boost efficiency. This work proposes a novel isolated soft-switching high step-up DC-DC converter. These DC-DC converters are connected cascaded at their output terminals to form the suggested inverter. When each DC-DC converter's output voltage is controlled, this inverter can function with high voltage gain. Additionally, it requires fewer DC-DC blocks to produce a greater range of output voltage levels. The suggested inverter is appropriate for photovoltaic power conditioning systems because of all these benefits.

Keywords: Multi-Phase Converter, Multi-Level Inverter, PV System, Current Controller, THD and DC-DC Converter

Introduction:

The quantity and strength of power electronics converters, which are becoming more and more common in commercial, industrial, and household settings, have grown dramatically in recent years. Switching is the primary activity in power electronics systems, and higher switching frequency values offer additional benefits.

Nevertheless, the power levels of inductive components and semiconductor power switches are limited

[1]. Generally speaking, power converters with less than 10 kW can employ high switching frequency values, but higher power levels require medium frequency values. High power converter design is therefore difficult. The restricted conversion rates of DC-DC converters are another issue. Despite their widespread use and simplicity, non-isolated DC-DC converters have a limited voltage conversion ratio [2]. Consequently, in applications where a high conversion ratio is necessary, isolated DC-DC converters with a transformer integrated into the converter construction are employed. They are also extensively utilised in the design of contemporary power systems, including uninterruptible power supplies and electric cars. In order to serve loads and deliver generated voltage to grid, renewable energy sources like fuel cells and photovoltaic modules need step-up converters with high gain values. These sources often produce lower voltage levels. Applications for isolated DC-DC converters with embedded medium frequency transformers have recently begun to be used in fuel cells, solar panels, wind turbines, and other renewable energy sources [3].

A transformer serves a variety of functions in a medium frequency power converter. This transformer's size and volume can be designed at medium frequency in a comparatively modest structure. Furthermore, smart grids and next-generation grids have gained popularity recently. Bi-directional isolated DC-DC power converter topologies are intended for distinct uses in these systems. Power transformers serve three purposes in these kinds of applications. The second objective is to use conversion rate to adjust the supply voltage level to the load voltage level [4]. As a result, the transformer's conversion ratio can be matched with the voltage level that is acquired from various energy sources. Bi-directional design is another option for this kind of DC-DC converter. With their benefits, isolated DC-DC converters are frequently explored for a variety of applications, including power supplies, traction applications, and renewable energy applications [5].

This paper proposes a five-phase, bidirectional DC-DC converter. In order to generate multi-phase, multi-level voltages on the primary side of a high frequency transformer. 1.7 kV silicon carbide MOSFETs are employed in this construction.

Proposed System Configuration:

Figure 1 depicts the suggested bidirectional isolated dc-dc converter with multi-phase. The primary converter for each phase is 5LMTC, as seen in this image. Since the transformer turn ratio restricts the voltage range of the secondary side, the standard

three-level T-type converter is used as the secondary converter. A bidirectional switch and a half bridge unit make up each 3LTC. In the suggested structure, the a-phase operates in the following ways:

First, by activating switches S1,a and S5,a, the 5LMTC generates a voltage of 2VH at the transformer's main side, and by activating switch T1,a, the 3LTC generates a voltage of VL at the transformer's secondary side. Second, the voltage at the transformer's primary side is VH, and switches S3,1,a, S3,2,a, and S5,a are all on in the 5LMTC [6]. Third, the primary and secondary voltages are zero, and switches S2,a, S5,a, T3,1,a, and T3,2,a are all on. In the negative half cycle, the same patterns are taken into account.

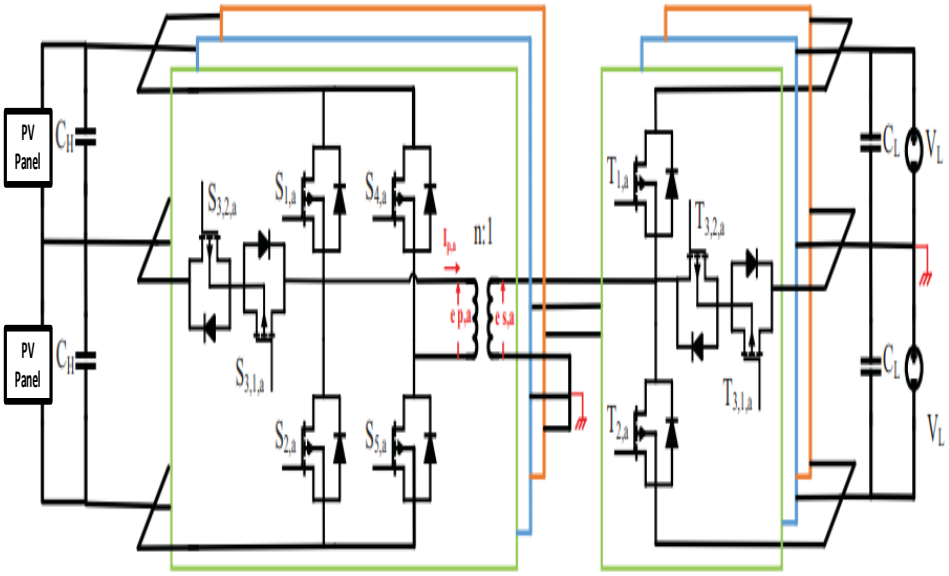

Figure 1: Proposed Five-Phase DC-DC Isolated Bidirectional Converter

PV Solar System:

Due to free in nature, dependability, and affordability, the solar system has played a key role in power generation systems. Due to photon effect, solar panel converts sun light into electrical energy [7]. Electric current flows initially from solar cells and is afterwards turned into voltage with the aid of an analogous electric circuit. The obtained DC voltage can damage electrical equipment and fluctuates based on the sun's temperature. The circuit diagram for an MPPT-based PV system with a DC-DC converter is displayed in Figure 2. Monitoring the maximum output of the solar panel is the aim of the MPPT [8].

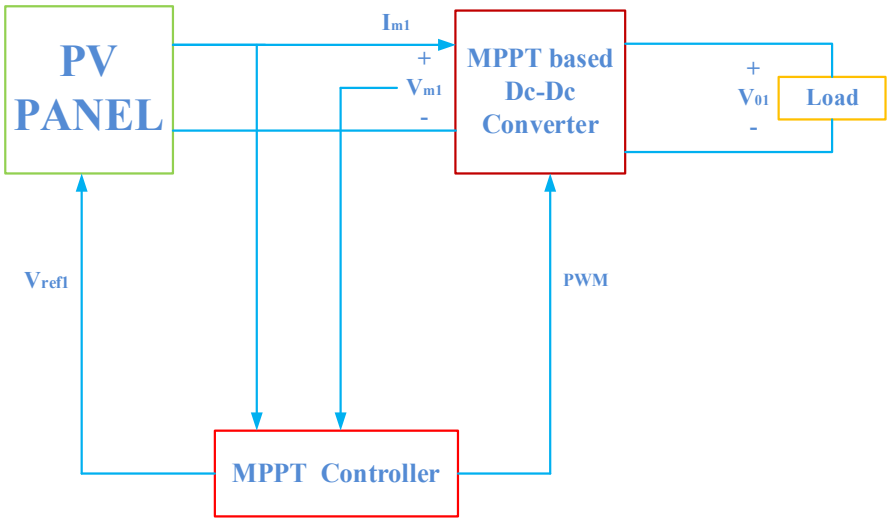

Figure 2: Solar System with MPPT based DC-DC Converter

Tracking solar system power is the goal of the MPPT approach. A rudimentary DC to DC converter with maximum power point tracker technique for pv system helps to improve the PV performance [9]. This converter's main functions are to regulate solar voltage and monitor panel output at its peak. Equation 1(a) & (b) shows the mathematical representation of PV current and Diode Currents. Figure 3 shows the equivalent diagram solar electrical circuit.

$$I_1 = I_{ph1} - I_{D1} - I_{sh1} \qquad (1.a)$$

$$I_1 = I_{ph} - I_o[e^{(\frac{qV_D}{nKT})}] - (\frac{V_D}{R_s}) \qquad (1.b)$$

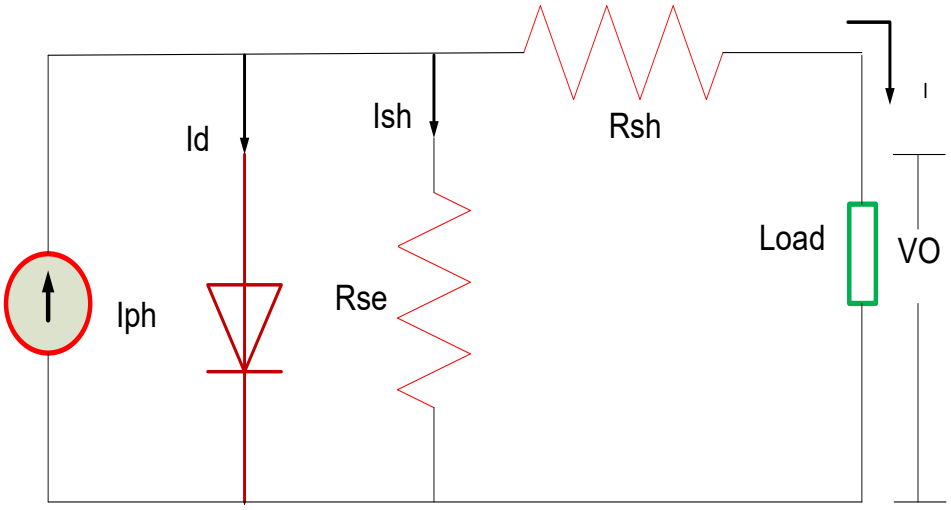

Figure 3: Electrical Equivalent Circuit

The mathematical expression for PV power is shown in equation 2

P=VI (2)

The expression of photovoltaic current in terms of temperature and solar irradiance is shown in equation (3)

$$I_{pha} = \left[I_{scra} + K_{1a}(T_{ea} - T_{ref}) \right] \frac{G}{G_{ref}} \qquad (3)$$

The expression for PV Current shown in (4)

$$I_{aa} = I_{pha} - I_{saa} \left[\exp(\frac{V}{\eta V_{ra}}) - 1 \right] - \left[\frac{V + IR_a}{R_{sha}} \right] \quad (4)$$

The expression for diode saturation current is expressed as (5),

$$I_{sa} = I_{RSa} (\frac{T_{ea}}{T_{ref}})^3 \exp\left[\frac{qE_g}{nk} \left(\frac{1}{T_{ref}} - \frac{1}{T_{ea}} \right) \right] \quad (5)$$

At reference temperature, the reverse saturation current can be roughly calculated as (6):

$$I_{Rsa} = \frac{I_{sca}}{\exp(\frac{qV_{oca}}{nkT_1}) - 1} \qquad (6)$$

Perturb and Observe MPPT Algorithm:

Optimization issues frequently arise in a wide range of scientific and technological fields. Due to model restrictions or the target function's practical implementation, these problems can occasionally be quite challenging [10]. An objective function with complex, nonlinear features and strong equality and/or equality restrictions is reduced or maximized in a typical optimization problem.

In the P&O method, system monitors changes in the array voltage before determining how the output power has changed. Figure 4 displays a P&O mppt algorithm. The PV power was computed in this flowchart after measuring the PV panel's voltage and current [11].

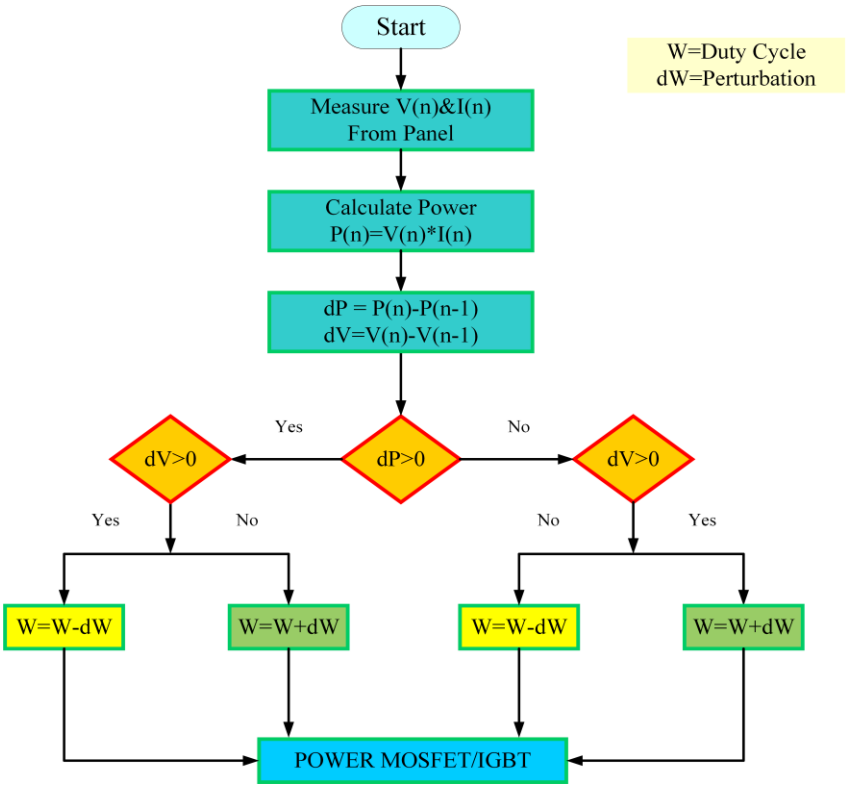

Figure 4: Flowchart representation of P&O technique

Closed Loop controller for DC-DC Converter:

The bidirectional converter is implemented with voltage signals in literature analysis for fast charging applications. But due to in compatibility of results, this paper designed a closed loop current controller to regulate the DC-DC converter. The converter and battery currents are chosen as reference signals for the controller. Figure 5, consists of three phases current source converter acts as a dc-link [12]. The three-phase inverter currents are expressed in terms of abc to dq transformation and made a comparison with reference current signals to generate required gate signals for converter.

$$i_{dqo} = T_{abc}^{dqo} i_{abc} \qquad (7)$$

$$T_{abc}^{dqo} = \frac{2}{3}\begin{bmatrix} \cos_n(wt) & \cos_n(wt-120^0) & \cos_n(wt+120^0) \\ -\sin_n(wt) & -\sin_n(wt-120^0) & -\sin_n(wt+120^0) \\ 0.5 & 0.5 & 0.5 \end{bmatrix}$$

$$L_{f1}\frac{di_{fdq1}}{dt} = -(R_{f1} + w_{dq}JL_{f1})i_{fdq1} - V_{cdq} + V_{dc}$$

$$L_{g1}\frac{di_{gdq1}}{dt} = -(R_{g1} + w_{dq}JL_{g1})i_{gdq1} + V_{cdq} - e_{gdq1}$$

$$C\frac{dV_{cdq1}}{dt} = -w_{dq}JCV_{cdq} + i_{fdq1} - i_{gdq1}$$

Here, the terms i_{fdq1} and i_{gdq1} are the inverter and transformer currents in terms of dq-transformation, w is angular frequency V_{cdq} is dc-link capacitor voltage [13]. R_{g1} and R_{f1} are the resistance in filter circuit of inverter side, L_{g1} and L_{f1} are the inverter filter currents.

Current Controller:

The proposed current controller for dc-dc converter for solar applications and three phase converters connected to grid through LCL filter helps to reduction of system dynamics [14]. The expression for reference current analysis is given in equation (10).

$$i(t)_{adq} = \frac{L_{f1} i(t)_{fdq1}}{L_{f1} + L_{g1}} + \frac{L_{g1} i(t)_{gdq1}}{L_{f1} + L_{g1}} \qquad (10)$$

Figure 5(a) shows the analysis of the closed-loop control diagram for the primary inverter current controller. Lf1 and Lg1 are filter inductors at the primary and secondary sides. By comparing reference current and actual current signals of d-axis and q-axis. Figure 5(b) shows the analysis of the closed-loop controller for the secondary inverter current controller. Lf1 and Lg1 are filter inductors at the primary and secondary sides [15].

Figure 6 shows the closed-loop controller for the PV battery converter. Here the rated battery current and rated converter current are compared with actual currents and identified. The reference Voltage (VL123) and battery bus voltage (Vz) use a conventional PI controller [16]. This reference voltage for PWM is determined, and the gate signals required for the bidirectional converter are generated.

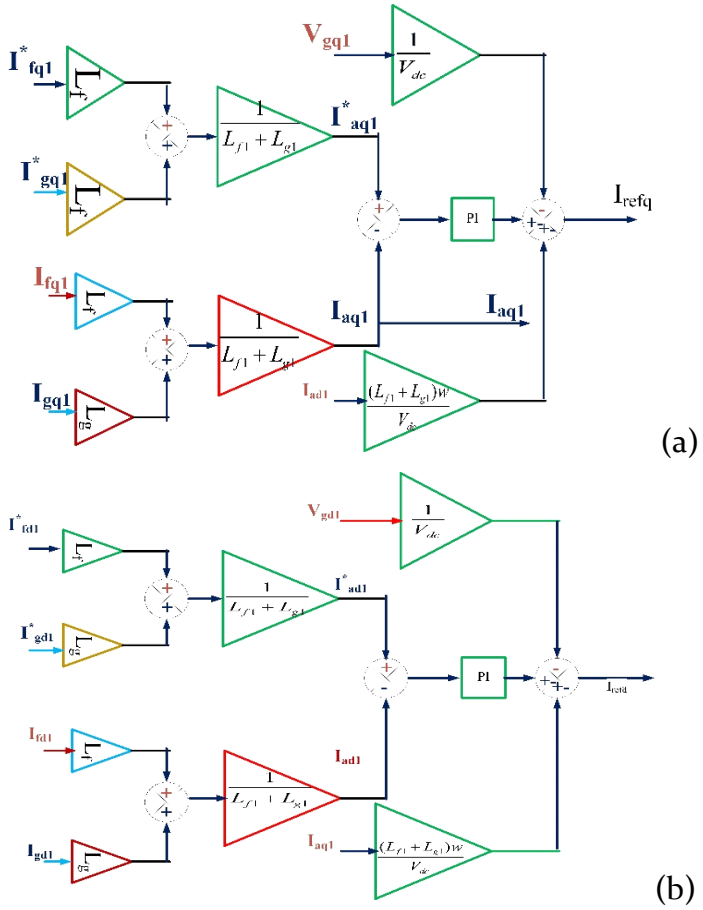

Figure 5: Closed loop controller for primary and secondary currents

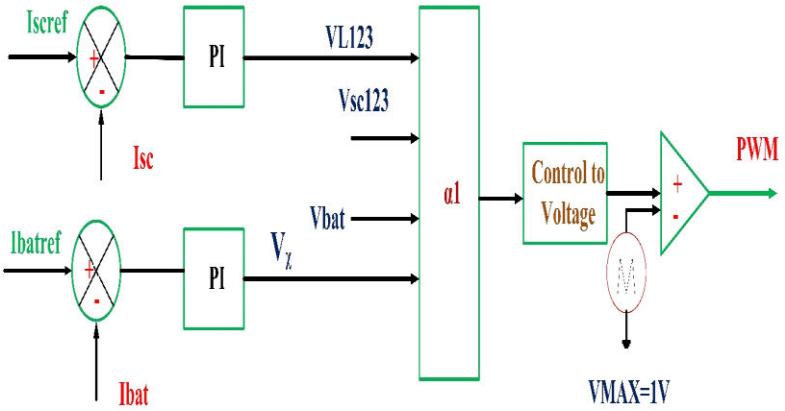

Figure 6: Closed Loop Current Controller for DC-DC Converter

Battery rated and actual currents are compared in order to construct the closed loop controller for the battery bi-directional converter, as illustrated in Figure 7 [17]. The controlled voltage is obtained from equation (11).

$$V_r^* = K_p(I_{bat1}^* - I_{bat1}) + K_i \int (I_{bat1}^* - I_{bat1}) \quad (11)$$

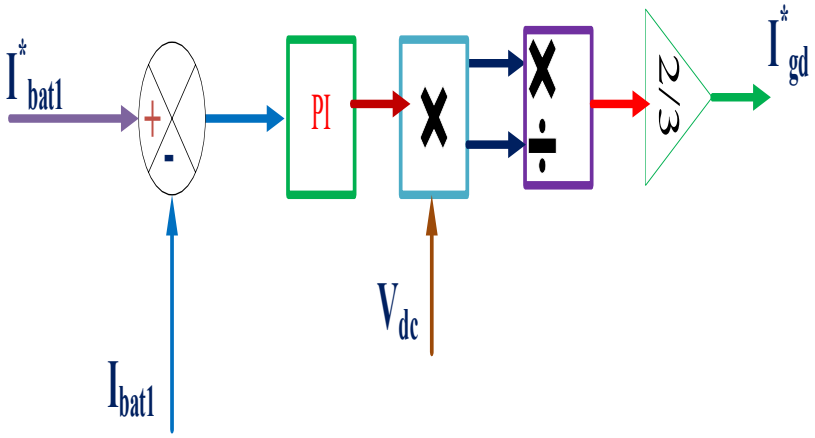

Figure 7: Closed Loop Control Diagram for

Switching Sequence of Interleaved Converter

The switching sequence for four IGBTs used in the dc-dc converter is shown in Figure 8. The switching period for four IGBT switches is represented as 'T,' and the expression for the switching period is shown below

Phase Shift = Ts/(no. of switches * no. of parallel phases) = Ts/4 (2)

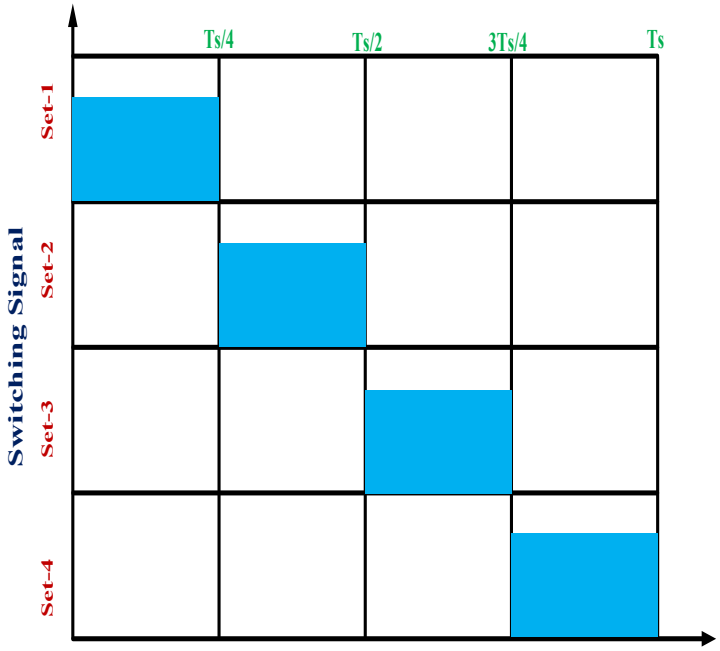

Figure 8: Switching Sequence

Space Vector Modulation

The two primary categories of basic modulation technique analysis for inverter circuit control are hysteresis controller and basic modulation technique. These controllers' primary drawback is that they add harmonic content to the inverter's voltage and current signals. This research suggests a space vector modulation approach notion to address this issue. Switches So and S7 serve as null vectors, whereas switching sequences S1 through S6 produce the gate signals needed for positive and negative pulses [18]. Figure 9 displays the vector diagram for the three phase space vector.

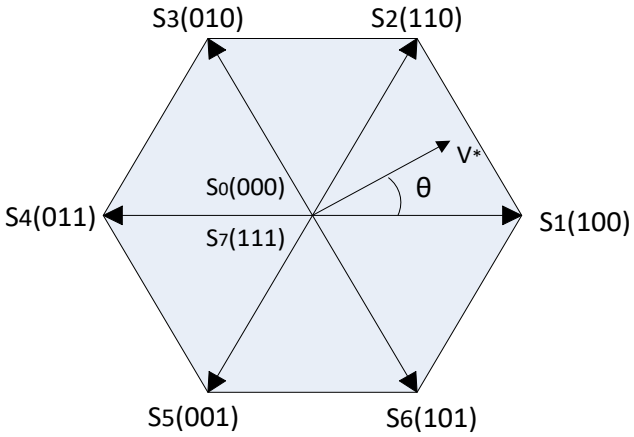

Figure 9: Six Vector Space Vector Modulation

The expression for generating reference voltage signal (V^*) and the pulse width time is shown in equation (3) [19],

(3)

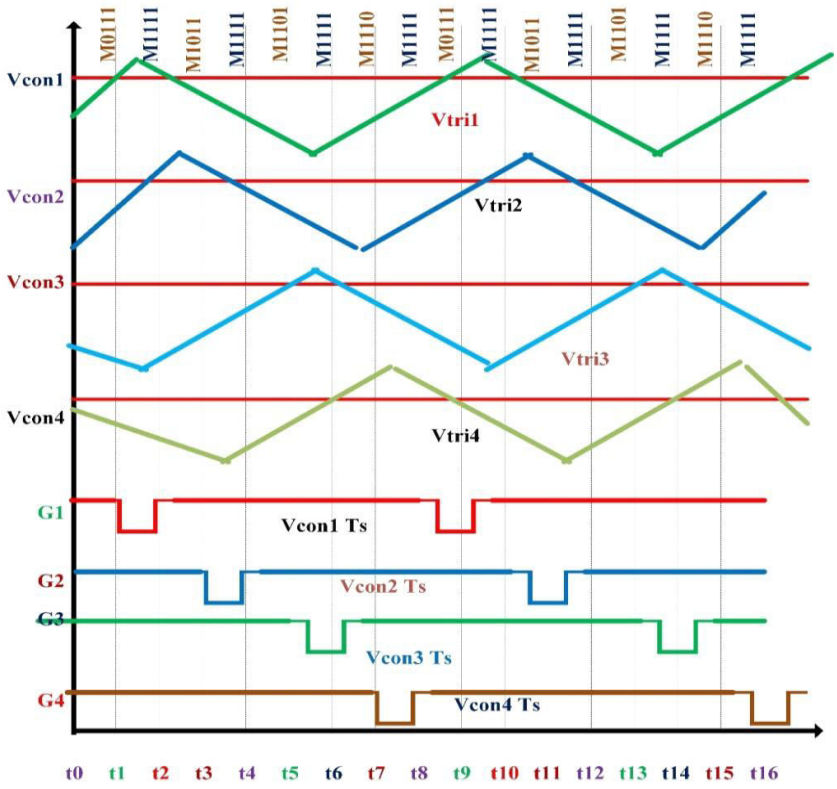

Figure 10: Illustrated waveforms

Simulation Analysis and Results:

The proposed system shown in figure 1 is designed and tested in MATLAB/Simulink and the required parameter specifications are shown in table-1.

Table 1: Converter Parameters

Parameter	Value
Input Voltage	100V
Output Voltage	24V
Capacitor @ Input	200uF
Leakage Inductance of transformer	25.4uH
Turns ratio of transformer	1:1
DC filter inductance	8.7mH
DC filter capacitance	10uF
Switching frequency	10KHz

Case 1: DC-DC Converter with Conventional closed loop controller

In this case the proposed PV fed DC-DC five phase bidirectional converter is implemented in MATLAB/Simulink as per the figure shown in 1. The parameters required for converter is shown in table-1. A conventional closed loop controller is designed to regulate the performance of converter. The specifications required for dc-dc bidirectional converter is shown in table-1.

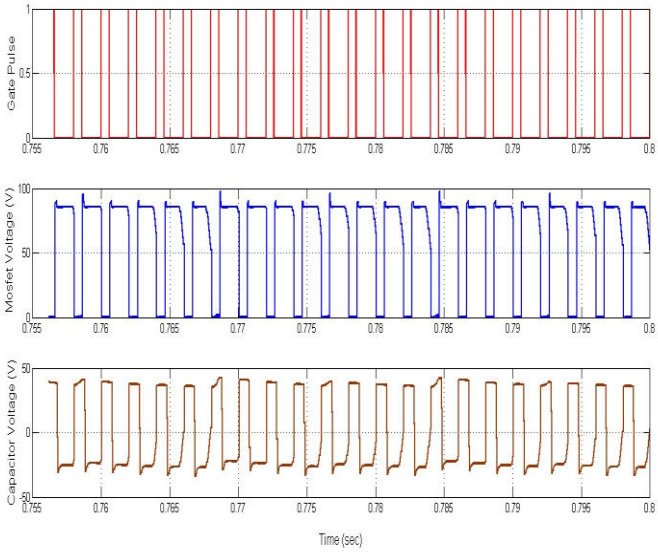

Figure 11: Simulation Waveform of Primary Parameters of DC-DC Converter

Figure 11, shows the switching pulses required for converter primary side, during this switching states the corresponding Mosfet voltage and capacitor voltage is measured and shown in figure 11.

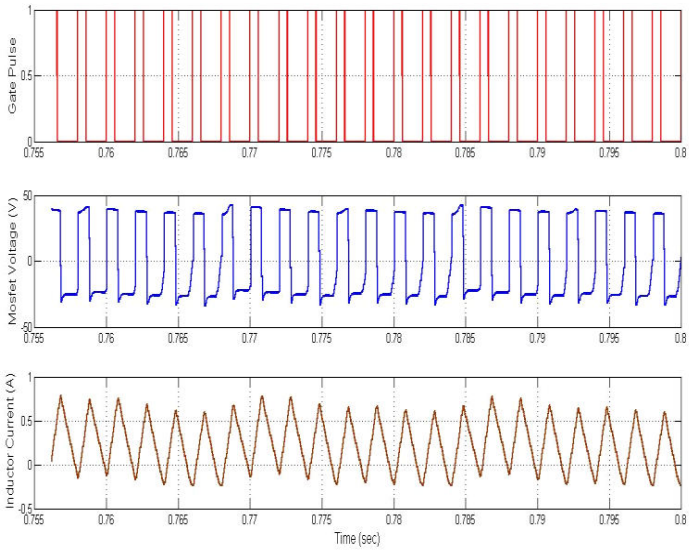

Figure 12: Simulation Waveform of DC-DC Converter Secondary Side

The simulation waveform for switching pulses required for secondary side converter is shown in figure 12. The secondary capacitor voltage and inductor current is obtained during this switching periods and shown in figure 12.

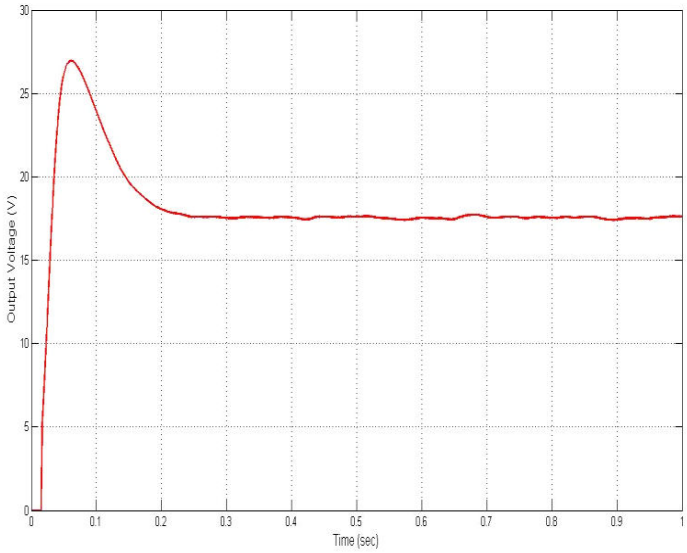

Figure 13: Simulation waveform for converter output voltage

The output voltage from the bidirectional converter with conventional controller is shown in figure 13. As from the waveform with an input volage of 100V, the converter produces an output voltage of only 22V. To improve the system performance a closed loop based current controller is designed, it also helps to improve the converter efficiency.

Case 2: DC-DC Converter with closed loop current controller

In this case the primary and secondary currents are taken consideration to generate the reference signal required for converter based on the figures shown in 5, 6 and 7.

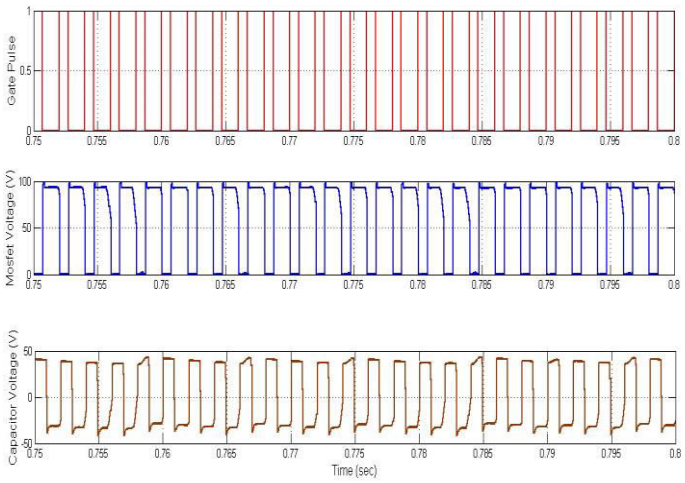

Figure 14: Simulation Waveform of Primary Parameters of DC-DC Converter

Figure 14, shows the switching pulses required for converter primary side, during this switching states the corresponding Mosfet voltage and capacitor voltage is measured and shown in figure 14.

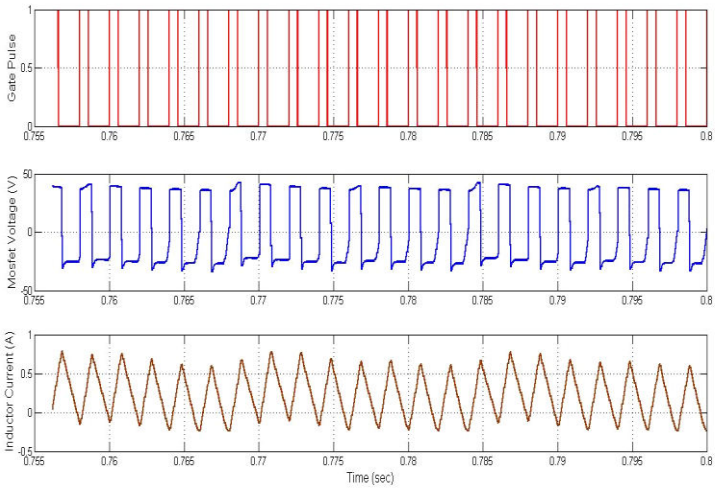

Figure 15: Simulation Waveform of Converter Secondary Side

Figure 15, shows the simulation waveform of output voltage and current for dc-dc converter secondary side with respect to gate pulses.

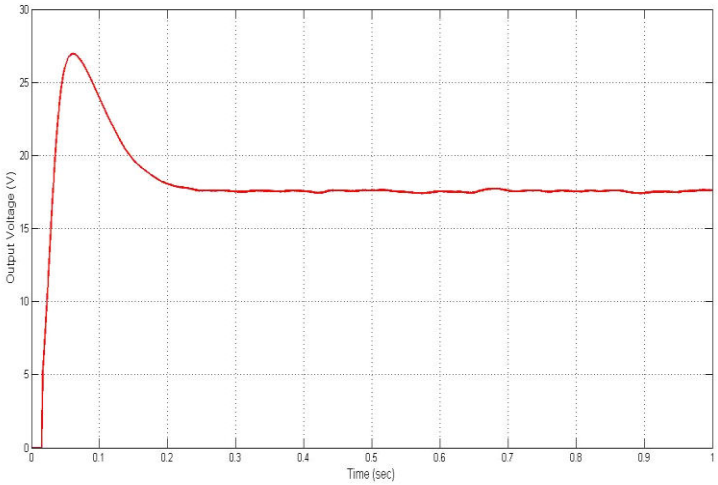

Figure 16: Waveform for converter output voltage

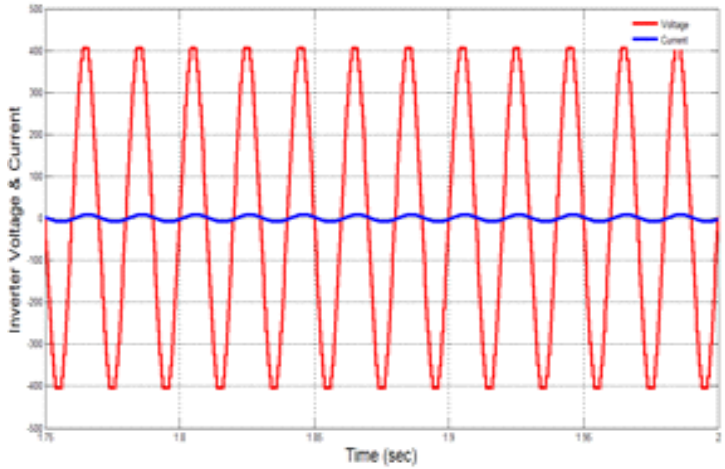

Figure 17: Multi-Level Voltage and current with RL load using conventional Controller

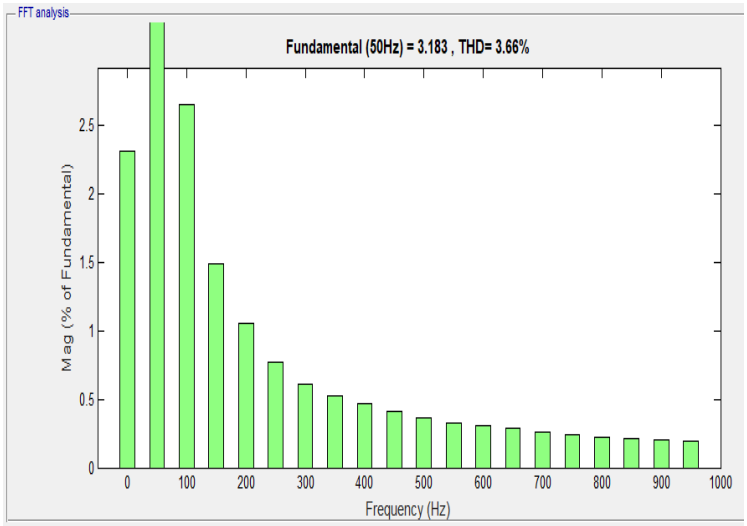

Figure 18: FFT Analysis for Inverter Voltage with RL Load

The output voltage from the proposed multi-level inverter under two case studies along with their corresponding harmonic distortions are shown from figure 17-20. Figure 17 and figure 18 shows the multi-level voltage and harmonic analysis, with the convention controller it shows 3.66% and by implementing a current based closed loop controller the harmonic distortions are better reduced to 2.23% as shown in figure 20.

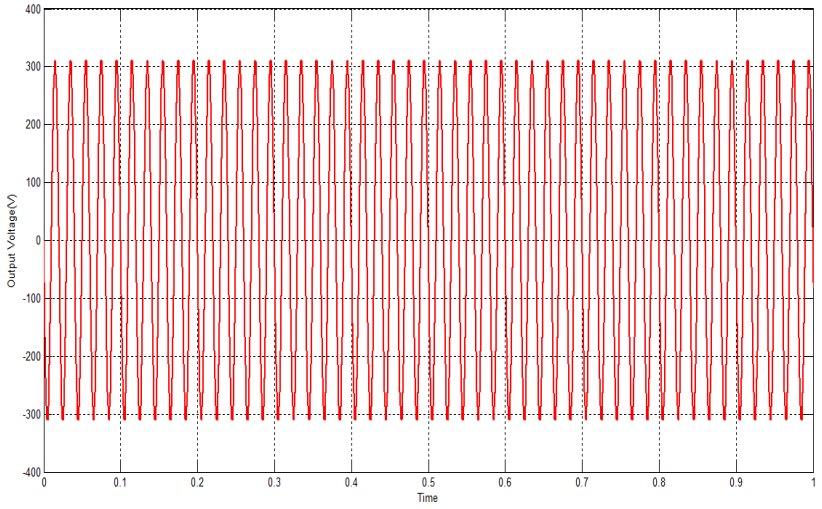

Figure 19: Multi-Level Voltage with RL load using Closed Loop Current Controller

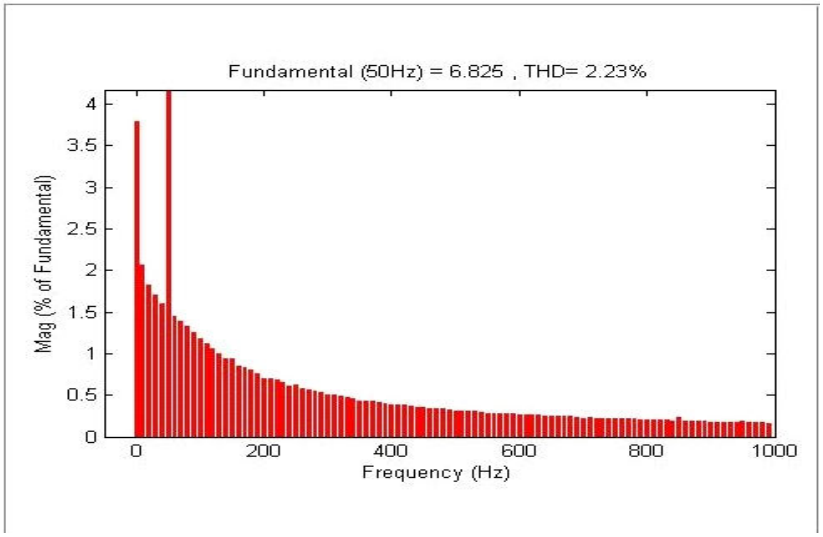

Figure 20: FFT Analysis for Inverter Voltage with RL Load

Conclusion:

In this paper, a closed loop controller based five-phase converter have proposed. The suggested five-phase converter reduces the size of the dc filter by creating multi-level voltage waveforms on the transformer's primary side based on the order in which the control switches are triggered. Furthermore, the suggested plan

eliminates power losses in the secondary side rectifier circuit by eliminating reverse recovery current in switches. To validate the suggested work, the efficiency of the suggested DC-DC SPS converter was contrasted with that of the current converter. The comparison revealed that the suggested converter with SPS has a greater efficiency than the current traditional controller-based DC-DC converter.

References:

1. A. J. Mason, D. J. Tschirhart, and P. K. Jain, "New ZVS phase shift modulated full bridge converter topologies with adaptive energy storage for SOFC application," IEEE Trans. Power Electron., Vol. 23, no. 1, pp. 332– 342, Jan. 2008.
2. J.-G. Cho, J.-W. Baek, C.-Y. Jeong, D.-W. Yoo, and K.-Y. Joe, "Novel Zero-Voltage and zero-current switching full bridge PWM converter using transformer auxiliary winding," IEEE Trans. Power Electron., Vol. 15, no. 2, pp. 250–257, Mar. 2000.
3. H. Cha, L. Chen, R. Ding, Q. Tang and F. Z. Peng, "An alternative energy recovery clamp circuit for full bridge PWM converters with wide ranges of input Voltage," IEEE Trans. Ind. Electron., Vol. 23, no. 6, pp. 2828– 2837, Nov, 2008.
4. Y. Jang and M. M Jovanovic, "A new PWM ZVS full bridge converter," IEEE Trans. Power Electron., Vol. 22, no. 3, pp. 987–994, May 2007.
5. P. K. Jain, W. Kang, H. Soin, and Y. Xi, "Analysis and design considerations of a load and line independent zero Voltage switching full-bridge DC/DC converter topology," IEEE Trans. Power Electron., Vol. 17, no. 5, pp. 649–657, Sep. 2002.
6. X. Wu, X. Xie, C. Zhao, Z. Qian, and R. Zhao, "Low Voltage and current stress ZVZCS full bridge dc–dc converter using center tapped rectifier reset," IEEE Trans. Ind. Electron., Vol. 55, no. 3, pp. 1470–1477, Mar. 2008.
7. W. J. Lee, C. E. Kim, G.W. Moon, and S. K. Han, "A new phase-shift full bridge converter with Voltage doubler-type rectifier for high-efficiency PDP sustaining power module," IEEE Trans. Ind. Electron., Vol. 55, no. 6, pp. 2450–2458, Jun. 2008.
8. S. Moissev, K. Konishi, S. Sato, L. Gamage, and M. Nakaoka, "Novel soft-commutation dc–dc power converter with high frequency transformer secondary side phase-shifted PWM active rectifier," IEE Proc. Electric Power Appl., Vol. 151, no. 3, May 2004.
9. X. Zhang, W. Chen, X. Ruan, and K. Yao, "A novel ZVS PWM phase shifted full-bridge converter with controlled auxiliary circuit," in Proc. IEEE Applied Power Electron. Conf., Feb. 2009, pp. 1067–1072.
10. H. Hamada and M. Nakaoka, "Analysis and design of a saturable reactor assisted soft-switching full-bridge dc– dc converter," IEEE Trans. Power Electron., Vol. 9, no. 3, pp. 309–317, May 1994.

11. J. Zhang, F. Zhang, X. Xie, D. Jiao, and Z. Qian, "A novel ZVS dc–dc converter for high power applications," IEEE Trans. Power Electron., Vol. 19, no. 2, pp. 420–429, Mar. 2004.
12. T. Mishima and M. Nakaoka, "Practical evaluations of A ZVS-PWM DC-DC converter with secondary-side phase-shifting active rectifier," IEEE Trans. Power Electron., Vol. 57, no. 99, pp. 1–12, Oct. 2011.
13. C. Yao, X. Ruan, X. Wang, and C. K. Tse, "Isolated buck–boost DC/DC converters suitable for wide input Voltage range," IEEE Trans. Power Electron., Vol. 26, no. 9, pp. 2599–2613, Sep. 2011.
14. M. A. Sayed, K. Suzuki, T. Takeshita, and W. Kitagawa, "PWM switching technique for three-phase bidirectional grid-tie dc-ac-ac converter with high frequency isolation," IEEE Trans. Power Electron., vol. PP, no. 99, pp. 1–1, 2017.
15. E.-H. Kim and B.-H. Kwon, "Zero-Voltage-and zero current-switching full-bridge converter with secondary resonance," IEEE Trans. Ind. Electron., Vol. 57, no. 3, pp. 1017–1025, Mar. 2010.
16. A. Sunil, G. E. Michael, and J. W. Michael, "Analysis and design of a new three-phase LCC-type resonant DC–DC converter with capacitor output filter," in Proc. IEEE Power Electron. Spec. Conf., 2000, pp. 721–728.
17. M. Almardy and A. K. S. Bhat, "Three-phase (LC)(L)- type series resonant converter: Design and experimental results," in Proc. Int. Conf. Electron. Devices, Syst. Appl., 2010, pp. 70–75.
18. D. S. Oliveira and I. Barbi, "A three-phase ZVS PWM DC/DC converter with asymmetrical duty cycle for high power applications," IEEE Trans. Power Electron., Vol. 20, no. 2, pp. 370–377, Mar. 2005.
19. F. Liu, G. Hu, and X. Ruan, "Three-phase three-level DC/DC converter for high input Voltage and high-power applications-adopting symmetrical duty cycle control," IEEE Trans. Power Electron., Vol. 29, no. 1, pp. 56– 65, Jan. 2014